











Radiomics Analysis of Gray-Scale Ultrasonographic Images of Papillary Thyroid Carcinoma > 1 cm: Potential Biomarker for the Prediction of Lymph Node Metastasis

Radiomics를 이용한 1 cm 이상의 갑상선 유두암의 초음파 영상 분석: 림프절 전이 예측을 위한 잠재적인 바이오마커

Hyun Jung Chung, MD¹ , Kyunghwa Han, PhD¹ , Eunjung Lee, PhD² , Jung Hyun Yoon, MD¹ , Vivian Youngjean Park, MD¹ , Minah Lee, MD¹ , Eun Cho, MD³ , Jin Young Kwak, MD^{1*} 


¹Department of Radiology, Severance Hospital, Research Institute of Radiological Science, Yonsei University College of Medicine, Seoul, Korea


²Department of Computational Science and Engineering, Yonsei University, Seoul, Korea

³Department of Radiology, Gyeongsang National University Changwon Hospital, Gyeongsang National University School of Medicine, Changwon, Korea

ORCID iDs

Hyun Jung Chung  <https://orcid.org/0000-0003-3910-167X>

Kyunghwa Han  <https://orcid.org/0000-0002-5687-7237>


Eunjung Lee  <https://orcid.org/0000-0001-9989-3555>

Jung Hyun Yoon  <https://orcid.org/0000-0002-2100-3513>

Vivian Youngjean Park  <https://orcid.org/0000-0002-5135-4058>

Minah Lee  <https://orcid.org/0000-0003-0175-4245>

Eun Cho  <https://orcid.org/0000-0001-7814-7430>

Jin Young Kwak  <https://orcid.org/0000-0002-6212-1495>

Received September 17, 2021

Revised March 9, 2022

Accepted April 19, 2022

*Corresponding author

Jin Young Kwak, MD
Department of Radiology,
Severance Hospital,
Research Institute of
Radiological Science,
Yonsei University
College of Medicine,
50-1 Yonsei-ro, Seodaemun-gu,
Seoul 03722, Korea.

Tel 82-2-2228-7400

Fax 82-2-2227-8337

E-mail docjin@yuhs.ac

This is an Open Access article distributed under the terms of the Creative Commons Attribution Non-Commercial License (<https://creativecommons.org/licenses/by-nc/4.0>) which permits unrestricted non-commercial use, distribution, and reproduction in any medium, provided the original work is properly cited.

Purpose This study aimed to investigate radiomics analysis of ultrasonographic images to develop a potential biomarker for predicting lymph node metastasis in papillary thyroid carcinoma (PTC) patients.

Materials and Methods This study included 431 PTC patients from August 2013 to May 2014 and classified them into the training and validation sets. A total of 730 radiomics features, including texture matrices of gray-level co-occurrence matrix and gray-level run-length matrix and single-level discrete two-dimensional wavelet transform and other functions, were obtained. The least absolute shrinkage

and selection operator method was used for selecting the most predictive features in the training data set.

Results Lymph node metastasis was associated with the radiomics score ($p < 0.001$). It was also associated with other clinical variables such as young age ($p = 0.007$) and large tumor size ($p = 0.007$). The area under the receiver operating characteristic curve was 0.687 (95% confidence interval: 0.616–0.759) for the training set and 0.650 (95% confidence interval: 0.575–0.726) for the validation set.

Conclusion This study showed the potential of ultrasonography-based radiomics to predict cervical lymph node metastasis in patients with PTC; thus, ultrasonography-based radiomics can act as a biomarker for PTC.

Index terms Papillary Thyroid Carcinoma; Ultrasonography; Lymphatic Metastasis; Biomarkers

INTRODUCTION

The incidence of thyroid malignancy continues to rise worldwide as ultrasonography (US) increases in use, enabling the detection of small cancers (1, 2). Papillary thyroid carcinoma (PTC) accounts for approximately 90% of thyroid malignancies (1). Often, PTC follows a relatively indolent and curable course, but disease persistence, recurrence, and even mortality still trouble PTC patients (1, 3, 4). Lymphatic spread is associated with the risk of regional recurrence, which leads to impairment of quality of life. Thus, identifying lymph node metastasis (LNM) preoperatively is crucial for the surgeons to plan optimal surgery for the patients (5).

Predictors of prognosis have been investigated with clinical, pathological, and molecular approaches. Known clinicopathologic factors are LNM, larger tumor size, aggressive histological subtype, extensive extrathyroidal invasion, vascular invasion and distant metastasis (6-8). V-raf murine sarcoma viral oncogene homolog B1 (BRAF^{V600E}) mutations and telomerase reverse transcriptase (TERT) promoter mutations have been studied as prognostic molecular markers (9-12). Unfortunately, to obtain pathologic and molecular markers, invasive procedures such as biopsy or surgery are necessary (1, 13).

Because malignant-appearing PTC more frequently has LNM, extrathyroidal invasion, and higher tumor, nodes, and metastasis (TNM) stage compared with benign-appearing PTC, US features can be useful prognostic factors (7, 8). In contrast to pathological or genomic approaches, US can obtain suspicious features of the lesions non-invasively before the surgery to predict prognosis (1, 8). However, this approach of using US to identify suspicious features is a qualitative analysis, which is subjective and varies by observer (14, 15). Thus, instead of solely depending on the visual interpretation of images, a quantitative and objective approach is needed.

As medical imaging tools have improved, high-throughput extraction of quantitative features has become possible, leading to the development of radiomics (16). Radiomics converts medical images into high-dimensional and mineable data. It has been used in subsequent data analysis for decision support (16). Some studies have taken research further by investigating the radiomics signature as a potential disease biomarker (17-22). To the best of our knowledge, US-based radiomics may be a stepping stone for a new non-invasive biomarker. There-

fore, the aim of this study was to use the radiomics analysis of US images to develop a radiomics signature as a potential biomarker for predicting LNM in patients with PTCs.

MATERIALS AND METHODS

ETHICS STATEMENT

The Institutional Review Board approved this retrospective study and required neither patient approval nor informed consent for our review of patient images and records (IRB No. 4-2016-0941).

STUDY POPULATION

From August 2013 to May 2014, 1621 of 1747 patients who underwent preoperative US were diagnosed with thyroid cancer. Among them, consecutive 1606 patients were found to have PTC. Of 1606 patients, 1175 were excluded if they had already undergone surgery for papillary thyroid microcarcinoma (PTMC) with a maximal diameter of less than 10 mm ($n = 1127$), if they did not have conventional PTC ($n = 45$), or if they were younger than 19 years old ($n = 3$). PTMC were excluded according to an indication of fine needle aspiration (FNA) biopsy for a thyroid nodule (23). The reason for limiting to conventional PTC was to select the study subject for the most frequent and homogenous group. Patients younger than 19 years old were excluded since children in thyroid carcinoma carry a unique set of clinical, pathologic, and molecular characteristics (24). In total, 431 patients were included in our study and US images for radiomics were available from all patients.

Total thyroidectomy was performed in patients with extrathyroidal extension, multifocality, bilaterality, or LNM on preoperative or intraoperative findings. Prophylactic bilateral central compartment lymph node dissection was performed in patients undergoing total thyroidectomy, and prophylactic unilateral central compartment dissection was performed in patients undergoing hemithyroidectomy. Lateral compartment dissection was performed only when lateral LNM was diagnosed on preoperative US-FNA or on an intraoperative frozen section. Central compartment dissection included the paratracheal, pretracheal, and prelaryngeal lymph nodes, and lateral compartment dissection included lymph nodes at levels II, III, IV and anterior V. Multifocality and central and lateral LNM status were reviewed from the original pathological reports without the authors having knowledge of US features.

ACQUISITION OF US DATA

All patients underwent preoperative US which was performed prospectively by one of eleven radiologists dedicated to thyroid imaging (seven fellows with 1 or 2 years of experience and four faculties with 6 to 15 years of experience) with a 5-to 12- MHz linear transducer (iU22, Philips Medical Systems, Bothell, WA, USA) and a 6-to 13- MHz linear transducer (EUB-7500, Hitachi Medical, Tokyo, Japan). All index tumors were routinely evaluated and captured in both transverse and longitudinal planes. A representative US image was selected for each patient by an experienced faculty (K.J.Y.) on the picture archiving and communication system and then the image was stored as a JPEG image. All lesions included in radiomics were based on one nodule per patient, and lesions with the longest plane diameter were included. Re-

gions of interest (ROIs) were drawn on all images along nodule borders blindly without knowledge of the pathological outcome of LNM by a senior radiologist (K.J.Y.) who had 20 years of subspecialty experience in thyroid imaging using the Paint program of Windows 7 (Microsoft Corporation, Redmond, WA, USA) (25, 26). Lastly, it was confirmed that the ROI was drawn on the pathology confirmed lesions.

IMAGE PROCESSING

Once a representative US image was determined, the ROI was also selected by an experienced radiologist. Then patient information was eliminated and the image was converted to a gray-scale intensity image by removing saturation and hue information while maintaining luminance. US images can vary greatly depending on the situation, so all intensity images were normalized by the Min-Max method (min 0, max 255) and expressed in the same range for a direct comparison between patients (Fig. 1) (27). To avoid altering the pixel intensity of images by drawing the ROI, all US images had two duplicates, one with and without ROI marks, as shown in Figs. 1A and 1B. Only ROI locational information was collected from the image with ROI marks (Fig. 2B), and ROI was segmented from the image without ROI marks (Fig. 2D).

RADIOMICS FEATURE EXTRACTION METHODOLOGY

We used in-house software with algorithms implemented in Matlab R2016a (Mathworks). A total of 730 radiomics features, including data from gray-level co-occurrence matrix (GLCM) and gray-level run-length matrix (GLRLM) texture matrices, single-level discrete 2D wavelet transform and other functions, were obtained from a single image (28). From the intensity image, histogram parameters were computed and extracted. Histogram parameters included entropy, mean, standard deviation, skewness, kurtosis, energy, mean absolute deviation, median, and root mean square. Each of these parameters represent unique characteristics on images and their analysis incorporates first-order statistics. For instance, entropy measures texture irregularity in the image; mean provides the echogenicity information of the US image by calculating the average value of pixel intensity; skewness measures the distribution asymmetry about the mean; and kurtosis shows the peakedness of the intensity distribution. Textural features were obtained from GLCM and GLRLM matrices. GLCM and GLRLM were calculated in four directions (0, 45, 90, 135 degree angle) with a distance of 1. Twenty-two textural parameters were computed from GLCM which are autocorrelation, cluster prominence,

Fig. 1. Image processing.

A-D. All US images had two duplicates, one without **(A)** and another with ROI marks **(B)**. All US images were normalized using the Min-Max method (min 0, max 255) **(C, D)** and expressed in the same range for a direct comparison across patients.

ROI = region of interest, US = ultrasonography

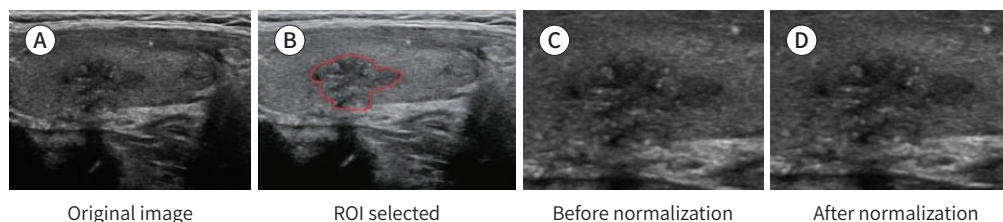
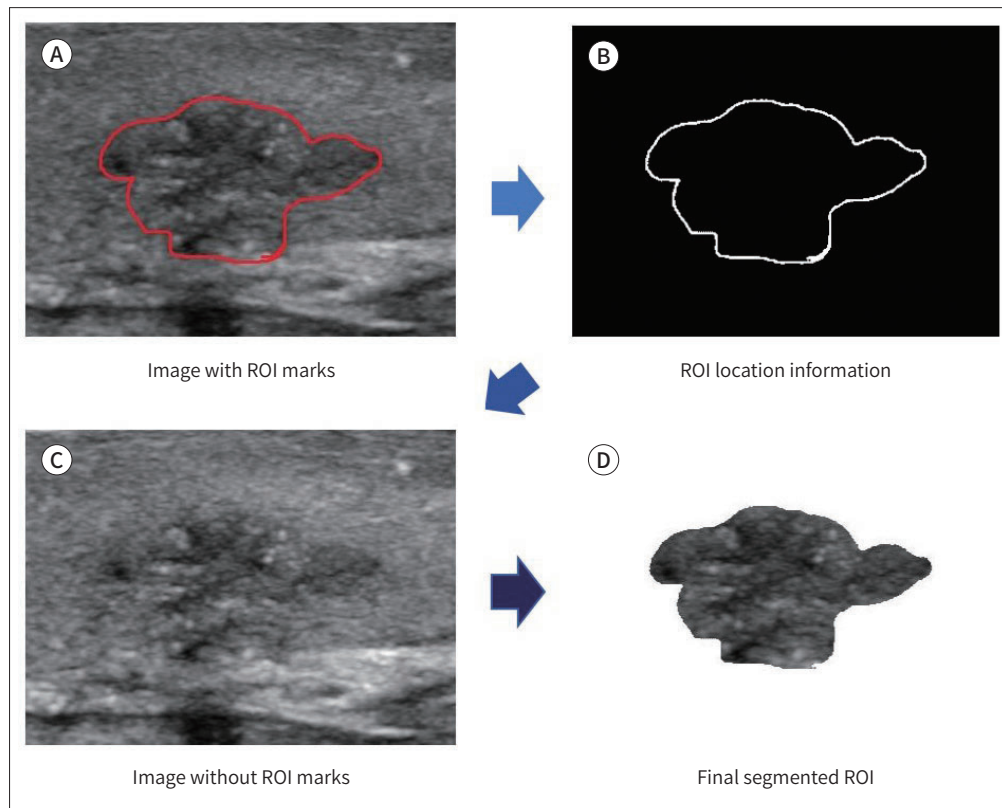


Fig. 2. The ROI segmentation process.

A-D. From the image with ROI marks (**A**), only the ROI locational information (**B**) is collected, and from the image without ROI marks (**C**), the ROI is segmented (**D**).

ROI = region of interest



cluster shade, cluster tendency, contrast, correlation, difference entropy, dissimilarity, energy, entropy, homogeneity, informational measure of correlation, inverse difference moment normalized, inverse difference normalized, inverse variance, maximum probability, sum average, sum entropy, sum variance and variance. GLRLM features consist of 11 parameters which are short run emphasis, long run emphasis, gray level non-uniformity, run length non-uniformity, run percentage, low gray level run emphasis, high gray level run emphasis, short run low gray level emphasis, short run high gray level emphasis, long run low gray level emphasis, and long run high gray level emphasis. Another set of the feature information was collected using wavelets. We used 2-space dimensional discrete one-level wavelet transformation to decompose the original US image using the 'coiflet 1' wavelet. For each direction, x- and y-directions, four discrete wavelet decompositions (LL, LH, HL, HH with H and L indicating a high-pass and low-pass filter in the x, y-directions, respectively) were sought. All of the previously introduced first-order statistics as well as GLCM- and GLRLM-related features were also calculated and extracted from these four wavelet applied images. Features were extracted using in-house codes implemented in MATLAB 2016b (MathWorks) (28).

STATISTICAL ANALYSIS

We randomly divided patients into two groups (a training set and a validation set) using

statistical software. Clinicopathologic variables were compared between the training and validation data set with the independent samples *t* test, Chi-square, or Fisher's exact test.

The least absolute shrinkage and selection operator (LASSO) method with 'glmnet' package, which is suitable for the regression of high-dimensional data, was used to select the most predictive features in the training data set (29). The final set of features were determined by 10-fold cross-validation. The cross-validated areas under the receiver operating characteristic curve (AUC) with standard errors were estimated according to the tuning parameter (λ) for LASSO. The λ value which narrowed the number of features into the final set was chosen to maximize the AUC. A radiomics score was calculated for each patient via a linear combination of the selected features weighted by their respective coefficients. Univariate and multivariate logistic regression analyses were performed to assess associations of LNM with clinical factors and the radiomics score. We evaluated the predictive abilities of the training data set and validation data set with AUCs. An AUC value of 1.0 indicated that patients with different results were divided completely, and a value of 0.5 indicated that the data yielded from our model was no different from data obtained at random. All statistical tests were two-sided, with a $p < 0.05$ considered significant. Statistical analyses were performed with R software, version 3.3.2 (<http://www.R-project.org>).

RESULTS

Out of total 431 patients, patients consisted of 320 (74.2%) female and 111 (25.8%) male. Mean patient age (\pm standard deviation) was 43.9 ± 13.3 years (range, 19–83 years). Mean female patient age was 43.3 ± 13.5 years (range, 19–83 years), and mean male patient age was 45.8 ± 12.4 years (range, 21–82 years). Mean cancer size was 15.8 ± 7.3 mm (range, 11–60 mm). Mean cancer size was 15.8 ± 7.3 mm (range, 11–60 mm).

The training data set included 216 patients (M:F = 56:160; mean age, 44.0 ± 13.3), and the validation data set included 215 patients (M:F = 55:160; mean age, 43.8 ± 13.4) (Table 1). The tumor size (mean, 16.6 ± 8.2 mm) of the training data set was larger than that (mean, 14.9 ± 6.2 mm) of the validation data set ($p = 0.017$). There were no significant differences between the data sets in terms of age, gender, multifocality, LNM, and distant metastasis.

Of texture features, 730 features were reduced to 1 potential predictor based on 216 pa-

Table 1. Patient Characteristics of the Training and Validation Data Sets

Characteristics	Training Data Set ($n = 216$)	Validation Data Set ($n = 215$)	<i>p</i> -Value
Age, years, mean \pm SD	44.0 ± 13.3	43.8 ± 13.4	0.888
Sex, %			0.193
Male	56 (25.9)	55 (25.6)	
Female	160 (74.1)	160 (74.4)	
Tumor size, mm, mean \pm SD	16.6 ± 8.2	14.9 ± 6.2	0.017
Multifocality, %	88 (40.7)	83 (38.6)	0.272
Lymph node metastasis, %	132 (61.1)	129 (60.0)	0.722
Distant metastasis, %	2 (0.9)	0 (0.0)	0.521

SD = standard deviation

Fig. 3. Texture feature selection using the LASSO binary logistic regression model.

A. Tuning parameter (Lambda) selection in the LASSO model used 10-fold cross-validation via maximum criteria. The AUC curve versus log (l) was plotted. Dotted vertical lines were drawn at the optimal values using the maximum criteria and one standard error of the minimum criteria (left: maximum; right: the one standard error criteria). An l value of 0.092, with log (l), -2.389 was chosen (maximum criteria) according to 10-fold cross-validation.

B. LASSO coefficient profiles of the 730 texture features are shown. A coefficient profile plot was produced against the log (l) sequence. A vertical line was drawn at the value selected using 10-fold cross-validation, where optimal l resulted in 24 nonzero coefficients. AUC = areas under the receiver operating characteristic curve, LASSO = least absolute shrinkage and selection operator

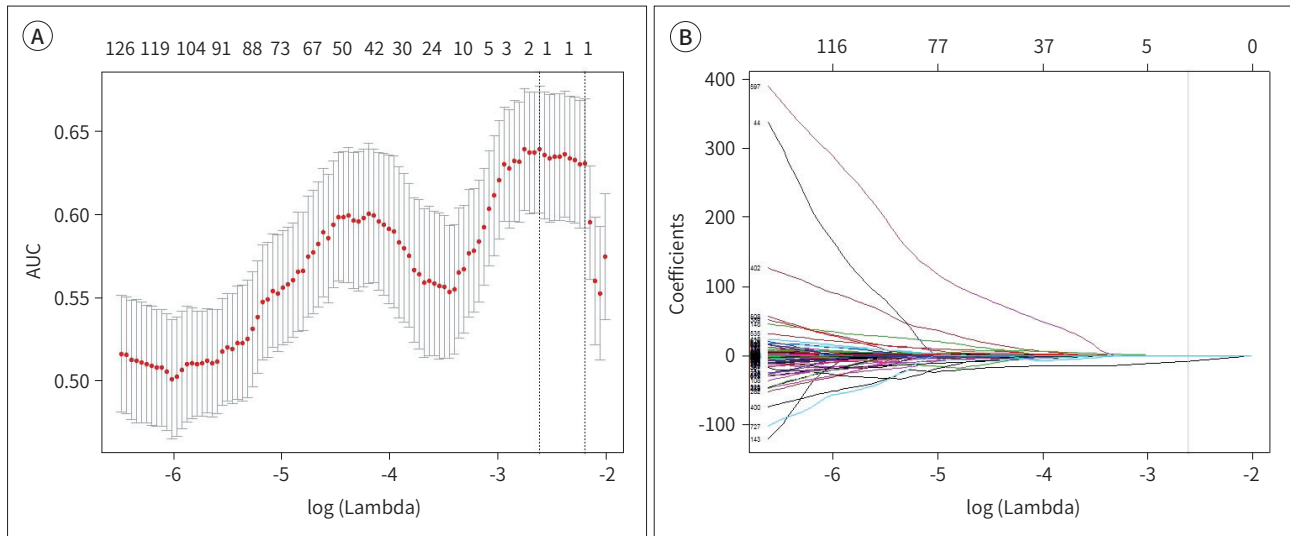


Table 2. Predictors of Lymph Node Metastasis in Patients with Papillary Thyroid Carcinoma Using Univariate and Multivariate Logistic Regression Analyses

	Crude Odds Ratio	p-Value	Adjusted Odds Ratio	p-Value
Age	0.973 (0.951-0.994)	0.013	0.969 (0.946-0.991)	0.007
Male sex	1.105 (0.586-2.119)	0.759	0.967 (0.487-1.940)	0.923
Tumor size	1.064 (1.019-1.129)	0.027	1.083 (1.026-1.154)	0.007
Radiomics score × 10 ²	1.082 (1.030-1.139)	0.002	1.099 (1.099-1.160)	< 0.001

Numbers in parentheses are 95% confidence intervals. Age, tumor size, and the radiomics score as continuous variables.

tients in the primary cohort (Figs. 3A, B), and these features had nonzero coefficients in the LASSO logistic regression model. They were presented in the Rad-score calculation formula, which was $1.416107 + HL_lgire_50_90 \times -2.0885729$. Table 2 shows the results of the univariate and multivariate analyses of clinical factors and radiomics score in the training data set to predict LNM. At univariate analysis, a higher radiomics score was statistically associated with an increased likelihood of LNM in PTC patients (95% confidence interval [CI], 1.030-1.139, $p = 0.002$). Among clinical variables, younger age (95% CI, 0.951-0.994, $p = 0.013$) and larger tumor size (95% CI, 1.019-1.129, $p = 0.027$) were significantly associated with a higher chance of LNM. At multivariate analysis, the radiomics score was independently associated with LNM (95% CI, 1.099-1.160, $p < 0.001$). LNM showed significant associations with other clinical variables such as younger age (95% CI, 0.946-0.991, $p = 0.007$) and larger tumor size (95% CI, 1.026-1.154, $p = 0.007$). AUC was 0.687 (95% CI: 0.616-0.759) for the training set, and 0.650 (95% CI: 0.575-0.726) for the validation set.

DISCUSSION

In this study, we presented a new way to predict LNM in patients with PTCs. Our study demonstrated utilizing the radiomics analysis of US images to obtain the radiomics score as a potential prognostic biomarker for LNM in patients with PTCs.

LNM is an important predictor of recurrence in PTC patients (7, 30, 31). Thus, accurate preoperative prediction of LNM is critical for making the best individualized treatment decision (32, 33). The high resolution of US has positioned it as the main diagnostic modality of LNM in patients with thyroid cancer, which also allows for accurate FNA of suspicious lymph nodes (1, 34, 35). However, US evaluation is limited by its subjectivity and operator dependency (25, 34). Thus, the use of objective quantitative imaging features with detailed analysis in clinical practice is being considered a possible alternative to subjective qualitative imaging features with interobserver variability (7, 25).

Deep learning with radiomics model has emerged as a technique that can realize the above goals by decoding clinical information such as tumor phenotype and genetic expression patterns and turning it into quantitatively mineable data (26, 34, 36). Previous study suggested the possibility of a feasible system to predict thyroid cancer recurrence using a deep learning model on US images (37). Specifically, the use of radiomics to predict disease prognosis, LNM in thyroid cancer has been investigated using computed tomography and US, with radiomics showing comparably high performance (Table 3) (25, 32, 34, 36, 38). A recent study on radiomics of thyroid carcinoma reported that the radiomics score showed better performance with higher AUC value than the junior radiologists in predicting malignancy of thyroid nodules (39). Accordingly, we evaluated whether radiomics could be used to predict cervical LNM in patients with PTCs.

In our study, the incidence of cervical LNM was 61.1% and 60.0%, respectively in the training data set and validation data set, which suggests that no significant differences exist between the two data sets. The radiomics score and other clinical variables such as younger age and larger tumor size were all statistically significant factors in this study. Among them, higher radiomics score was independently associated with cervical LNM in patient with PTCs.

As for our analytical results, among 730 radiomics features, HL-lglre_50_90 was selected as

Table 3. Studies on Radiomics for Predicting LNM in Patients with Papillary Thyroid Cancer

References	Modality	Prediction	Number of Total Patients	Number of Radiomics Features	Training Set AUC	Validation Set AUC
Lu et al. (34)	CT	Cervical LNM*	221	546 (8)	0.867	0.822
Zhou et al. (36)	DECT	Cervical LNM	108	223 (5)	0.910	0.847
Liu et al. (38)	US	Cervical LNM	450	614 (50)	0.782	0.727
Park et al. (25)	US	Lateral LNM [†]	400	730 (14)	0.710	0.621
Zhou et al. (32)	US	Central LNM [‡]	609	50 (23)	0.870	0.858

Numbers in parentheses are the number of selected radiomics features.

*Cervical lymph node (central and lateral lymph nodes of thyroid) metastasis is predicted.

[†] Only lateral lymph node metastasis is predicted.

[‡] Only central lymph node metastasis is predicted.

AUC = areas under the receiver operating characteristic curve, DECT = dual-energy CT, LNM = lymph node metastasis, US = ultrasonography

a statistically significant feature through the LASSO statistical technique. The extracted feature, *lgldre* (low gray level run emphasis), measures the distribution of low gray level values in adjacent or consecutive pixels/voxels of a single gray level in a given direction, with higher values indicating a greater concentration of low gray level values in the image. In other words, '*lgldre*' takes into account both pixel intensity and spatial relationships of the selected image. If the above mentioned value of *lgldre_50_90* is substituted into the radiomics score ($1.416107 + HL_lgldre_50_90 \times -2.0885729$) and calculated, it can be used to predict LNM. The predictive diagnostic accuracy of the validation set showed robustness in internal validation when compared to the performance of the radiomics signature in the training set.

Our results show that US-based radiomics may have the potential to provide the basis for a new non-invasive biomarker, but currently its discriminatory performance is not yet high enough to predict cervical LNM. Furthermore, in several other studies, the consideration of how to use radiomics in clinical settings continues. Although the utility of radiomics itself is important, research results are also being reported that when radiomics are used as a complementary tool in the medical field, they can play a role in securing the limitations of subjectivity and operator dependency of US. When radiomics are used together with US in clinical situations, the possibility of missing additional cancer can be reduced, so complementary use of radiomics can play a role in clinical settings (40).

This study has several limitations. First, data were collected retrospectively, and this might have created an inevitable selection bias. Second, lateral compartment neck node dissection was performed when the preoperative FNA or intraoperative frozen biopsy results showed lateral LNM, which might have caused LNM to be underestimated. Third, external validation was not performed using an independent data set from outside institutions, which might have caused overfitting. Finally, images obtained for the study were taken from multiple different types of US machines, which could have affected the radiomics features, and furthermore our results. However, our results also show that different types of US machines can be used to build US-based radiomics signatures, which opens the door for wider clinical application.

In conclusion, our study showed that US radiomics features of the primary tumor were associated with cervical LNM status in patients with PTCs. Although its accuracy is not yet high enough in the validation set, our results showed the possibility of the US-based radiomics application to clinical setting to predict cervical LNM in patients with PTCs, thus acting as a potential biomarker.

Author Contributions

Conceptualization, all authors; data curation, K.J.Y., H.K., L.E.; formal analysis, H.K., L.E.; funding acquisition, K.J.Y.; investigation, K.J.Y.; methodology, all authors; project administration, K.J.Y.; resources, K.J.Y.; software, K.J.Y., L.E.; supervision, K.J.Y.; validation, C.H.J., H.K., L.E., K.J.Y.; visualization, all authors; writing—original draft, C.H.J., K.J.Y.; and; writing—review & editing, C.H.J., K.J.Y.

Conflicts of Interest

The authors have no potential conflicts of interest to disclose.

Funding

This study was supported by the National Research Foundation of Korea (NRF) grant funded by the Korean government (MSIT) (2019R1A2C1002375 and 2021R1A2C2007492). The funders had no role in study design, data collection and analysis, decision to publish, or preparation of the manuscript.

REFERENCES

1. Haugen BR, Alexander EK, Bible KC, Doherty GM, Mandel SJ, Nikiforov YE, et al. 2015 American Thyroid Association management guidelines for adult patients with thyroid nodules and differentiated thyroid cancer: the American Thyroid Association Guidelines Task Force on thyroid nodules and differentiated thyroid cancer. *Thyroid* 2016;26:1-133
2. Davies L, Welch HG. Increasing incidence of thyroid cancer in the United States, 1973-2002. *JAMA* 2006;295:2164-2167
3. Sherman SI, Angelos P, Ball DW, Beenken SW, Byrd D, Clark OH, et al. Thyroid carcinoma. *J Natl Compr Canc Netw* 2005;3:404-457
4. Sherman SI, Brierley JD, Sperling M, Ain KB, Bigos ST, Cooper DS, et al. Prospective multicenter study of thyrocarcinoma treatment: initial analysis of staging and outcome. National Thyroid Cancer Treatment Cooperative Study Registry Group. *Cancer* 1998;83:1012-1021
5. Sakorafas GH, Sampanis D, Safioleas M. Cervical lymph node dissection in papillary thyroid cancer: current trends, persisting controversies, and unclarified uncertainties. *Surg Oncol* 2010;19:e57-e70
6. Furtado Mde S, Rosario PW, Calsolari MR. Persistent and recurrent disease in patients with papillary thyroid carcinoma with clinically apparent (cN1), but not extensive, lymph node involvement and without other factors for poor prognosis. *Arch Endocrinol Metab* 2015;59:285-291
7. Kim SY, Kwak JY, Kim EK, Yoon JH, Moon HJ. Association of preoperative US features and recurrence in patients with classic papillary thyroid carcinoma. *Radiology* 2015;277:574-583
8. Nam SY, Shin JH, Han BK, Ko EY, Ko ES, Hahn SY, et al. Preoperative ultrasonographic features of papillary thyroid carcinoma predict biological behavior. *J Clin Endocrinol Metab* 2013;98:1476-1482
9. Kim TH, Kim YE, Ahn S, Kim JY, Ki CS, Oh YL, et al. TERT promoter mutations and long-term survival in patients with thyroid cancer. *Endocr Relat Cancer* 2016;23:813-823
10. Xing M, Alzahrani AS, Carson KA, Shong YK, Kim TY, Viola D, et al. Association between BRAF V600E mutation and recurrence of papillary thyroid cancer. *J Clin Oncol* 2015;33:42-50
11. Liu X, Qu S, Liu R, Sheng C, Shi X, Zhu G, et al. TERT promoter mutations and their association with BRAF V600E mutation and aggressive clinicopathological characteristics of thyroid cancer. *J Clin Endocrinol Metab* 2014;99:E1130-E1136
12. Xing M, Liu R, Liu X, Murugan AK, Zhu G, Zeiger MA, et al. BRAF V600E and TERT promoter mutations cooperatively identify the most aggressive papillary thyroid cancer with highest recurrence. *J Clin Oncol* 2014;32:2718-2726
13. Ryoo I, Kwon H, Kim SC, Jung SC, Yeom JA, Shin HS, et al. Metabolomic analysis of percutaneous fine-needle aspiration specimens of thyroid nodules: potential application for the preoperative diagnosis of thyroid cancer. *Sci Rep* 2016;6:30075
14. Choi SH, Kim EK, Kwak JY, Kim MJ, Son EJ. Interobserver and intraobserver variations in ultrasound assessment of thyroid nodules. *Thyroid* 2010;20:167-172
15. Park CS, Kim SH, Jung SL, Kang BJ, Kim JY, Choi JJ, et al. Observer variability in the sonographic evaluation of thyroid nodules. *J Clin Ultrasound* 2010;38:287-293
16. Gillies RJ, Kinahan PE, Hricak H. Radiomics: images are more than pictures, they are data. *Radiology* 2016;278:563-577
17. Huang YQ, Liang CH, He L, Tian J, Liang CS, Chen X, et al. Development and validation of a radiomics nomogram for preoperative prediction of lymph node metastasis in colorectal cancer. *J Clin Oncol* 2016;34:2157-2164
18. Huang Y, Liu Z, He L, Chen X, Pan D, Ma Z, et al. Radiomics signature: a potential biomarker for the prediction of disease-free survival in early-stage (I or II) non-small cell lung cancer. *Radiology* 2016;281:947-957
19. Coroller TP, Agrawal V, Narayan V, Hou Y, Grossmann P, Lee SW, et al. Radiomic phenotype features predict pathological response in non-small cell lung cancer. *Radiother Oncol* 2016;119:480-486
20. Huynh E, Coroller TP, Narayan V, Agrawal V, Hou Y, Romano J, et al. CT-based radiomic analysis of stereotactic body radiation therapy patients with lung cancer. *Radiother Oncol* 2016;120:258-266
21. Cameron A, Khalvati F, Haider MA, Wong A. MAPS: a quantitative radiomics approach for prostate cancer detection. *IEEE Trans Biomed Eng* 2015;63:1145-1156
22. Parmar C, Leijenaar RT, Grossmann P, Rios Velazquez E, Bussink J, Rietveld D, et al. Radiomic feature clus-

- ters and prognostic signatures specific for lung and head & neck cancer. *Sci Rep* 2015;5:11044
23. Feldkamp J, Führer D, Luster M, Musholt TJ, Spitzweg C, Schott M. Fine needle aspiration in the investigation of thyroid nodules. Indications, procedures and interpretation. *Dtsch Arztebl Int* 2016;113:353-359
 24. Paulson VA, Rudzinski ER, Hawkins DS. Thyroid cancer in the pediatric population. *Genes* 2019;10:723
 25. Park VY, Han K, Kim HJ, Lee E, Youk JH, Kim EK, et al. Radiomics signature for prediction of lateral lymph node metastasis in conventional papillary thyroid carcinoma. *PLoS One* 2020;15:e0227315
 26. Park VY, Han K, Lee E, Kim EK, Moon HJ, Yoon JH, et al. Association between radiomics signature and disease-free survival in conventional papillary thyroid carcinoma. *Sci Rep* 2019;9:4501
 27. Li Y, Han G, Wu X, Li ZH, Zhao K, Zhang Z, et al. Normalization of multicenter CT radiomics by a generative adversarial network method. *Phys Med Biol* 2021;66:055030
 28. Aerts HJ, Velazquez ER, Leijenaar RT, Parmar C, Grossmann P, Carvalho S, et al. Decoding tumour phenotype by noninvasive imaging using a quantitative radiomics approach. *Nat Commun* 2014;5:4006
 29. Friedman J, Hastie T, Tibshirani R. Regularization paths for generalized linear models via coordinate descent. *J Stat Softw* 2010;33:1-22
 30. Mansour J, Sagiv D, Alon E, Talmi Y. Prognostic value of lymph node ratio in metastatic papillary thyroid carcinoma. *J Laryngol Otol* 2018;132:8-13
 31. Siddiqui S, White MG, Antic T, Grogan RH, Angelos P, Kaplan EL, et al. Clinical and pathologic predictors of lymph node metastasis and recurrence in papillary thyroid microcarcinoma. *Thyroid* 2016;26:807-815
 32. Zhou SC, Liu TT, Zhou J, Huang YX, Guo Y, Yu JH, et al. An ultrasound radiomics nomogram for preoperative prediction of central neck lymph node metastasis in papillary thyroid carcinoma. *Front Oncol* 2020;10:1591
 33. Tian X, Song Q, Xie F, Ren L, Zhang Y, Tang J, et al. Papillary thyroid carcinoma: an ultrasound-based nomogram improves the prediction of lymph node metastases in the central compartment. *Eur Radiol* 2020;30:5881-5893
 34. Lu W, Zhong L, Dong D, Fang M, Dai Q, Leng S, et al. Radiomic analysis for preoperative prediction of cervical lymph node metastasis in patients with papillary thyroid carcinoma. *Eur J Radiol* 2019;118:231-238
 35. Kwak JY, Han KH, Yoon JH, Moon HJ, Son EJ, Park SH, et al. Thyroid imaging reporting and data system for US features of nodules: a step in establishing better stratification of cancer risk. *Radiology* 2011;260:892-899
 36. Zhou Y, Su GY, Hu H, Ge YQ, Si Y, Shen MP, et al. Radiomics analysis of dual-energy CT-derived iodine maps for diagnosing metastatic cervical lymph nodes in patients with papillary thyroid cancer. *Eur Radiol* 2020;30:6251-6262
 37. Kil J, Kim KG, Kim YJ, Koo HR, Park JS. Deep learning in thyroid ultrasonography to predict tumor recurrence in thyroid cancers. *J Korean Soc Radiol* 2020;81:1164-1174
 38. Liu T, Zhou S, Yu J, Guo Y, Wang Y, Zhou J, et al. Prediction of lymph node metastasis in patients with papillary thyroid carcinoma: a radiomics method based on preoperative ultrasound images. *Technol Cancer Res Treat* 2019;18:1533033819831713
 39. Liang J, Huang X, Hu H, Liu Y, Zhou Q, Cao Q, et al. Predicting malignancy in thyroid nodules: radiomics score versus 2017 American College of Radiology Thyroid Imaging, Reporting and Data System. *Thyroid* 2018;28:1024-1033
 40. Park VY, Lee E, Lee HS, Kim HJ, Yoon J, Son J, et al. Combining radiomics with ultrasound-based risk stratification systems for thyroid nodules: an approach for improving performance. *Eur Radiol* 2021;31:2405-2413

Radiomics를 이용한 1 cm 이상의 갑상선 유두암의 초음파 영상 분석: 림프절 전이 예측을 위한 잠재적인 바이오마커

정현정¹ · 한경화¹ · 이은정² · 윤정현¹ · 박영진¹ · 이민아¹ · 조 은³ · 곽진영^{1*}

목적 갑상선 유두암 환자에서 림프절 전이를 예측할 수 있는 잠재적인 바이오마커를 개발하기 위해 초음파 영상에 대한 radiomics를 조사하는 것이다.

대상과 방법 2013년 8월부터 2014년 5월까지 431명의 환자가 연구에 포함되었고 통계 소프트웨어를 사용하여 훈련 및 검증 세트로 구분되었다. 총 730개의 radiomics 특징이 자동으로 추출되었다. 훈련 데이터 세트에서 가장 예측 가능한 특징을 선택하기 위해 최소 절대 수축 및 선택 연산자가 사용되었다.

결과 Radiomics 점수는 림프절 전이와 관련이 있었다($p < 0.001$). 림프절 전이는 젊은 연령($p = 0.007$) 및 더 큰 종양 크기($p = 0.007$)와 같은 다른 임상 변수와도 관련이 있었다. 수신자 조작 특성 곡선 하 면적 결과 값은 훈련 세트의 경우 0.687 (95% 신뢰 구간: 0.616–0.759), 검증 세트의 경우 0.650 (95% 신뢰 구간: 0.575–0.726)이었다.

결론 본 연구 결과는 초음파 영상 기반의 radiomics가 papillary thyroid carcinoma 환자에게서 경부 림프절 전이를 예측하고 바이오마커로 작용할 가능성을 보여주었다.

¹연세대학교 의과대학 세브란스병원 방사선과학연구소 영상의학과,

²연세대학교 전산과학공학교실,

³경상대학교 의과대학 경상대학교창원병원 영상의학과